

Supplementary Information of
Tunable Opto-Magnetic Metamaterials via Coupled TiN-NiO Vertically Aligned
Nanocomposite Thin Films

Natalia Garcia Godinez¹, Jiawei Song¹, Yizhi Zhang¹, Amirr Dion Neal¹, Claire Mihalko¹,
Lizabeth Quigley¹, Juanjuan Lu¹, Ping Lu^{2,3}, Haiyan Wang^{1,4}

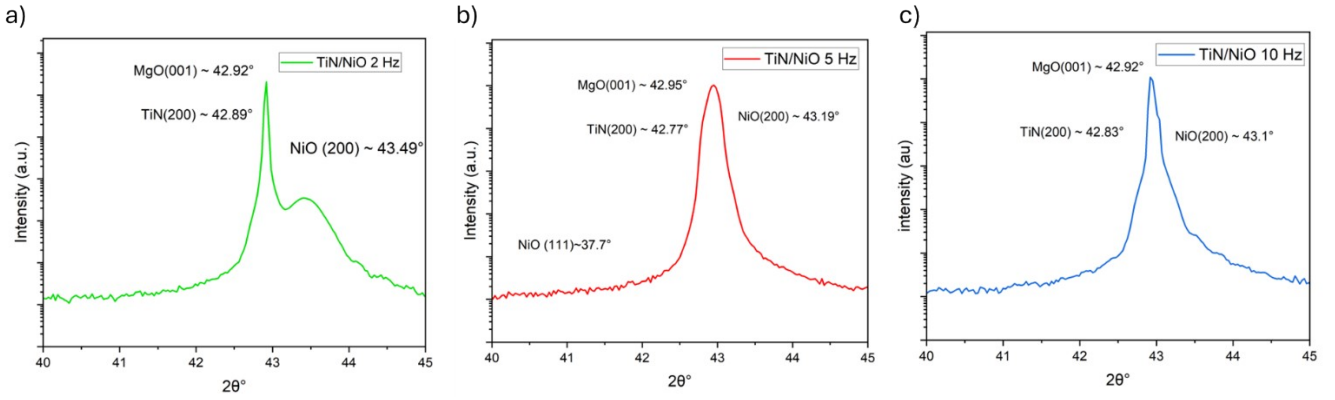
¹ School of Materials Engineering, Purdue University, West Lafayette, Indiana 47907, USA

² Sandia National Laboratory, Albuquerque, New Mexico 87185, USA

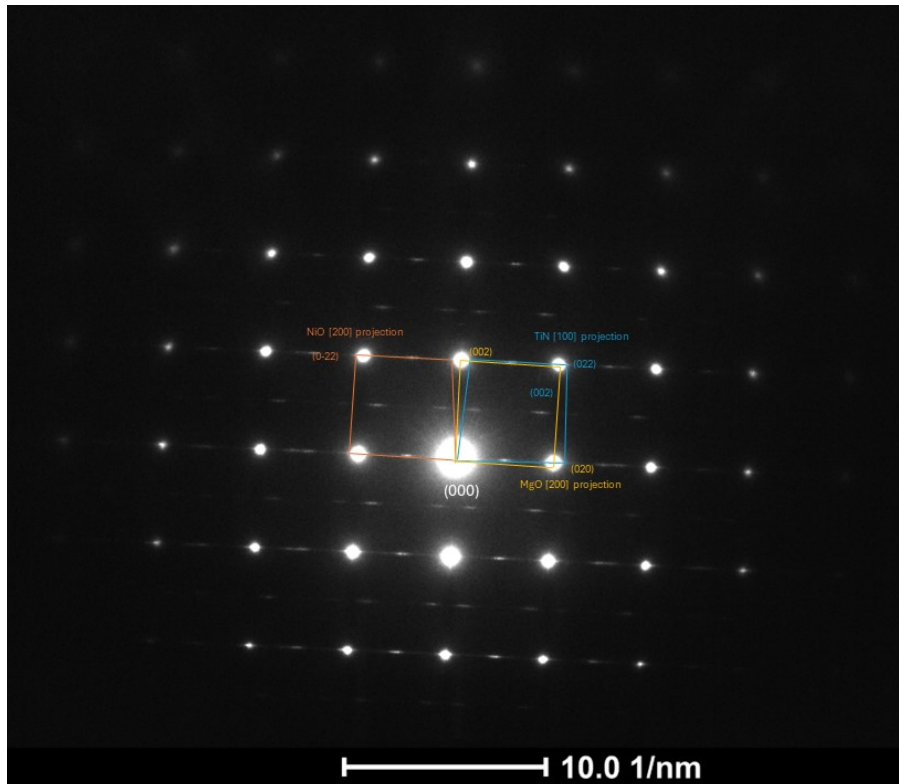
³ Center for Integrated Nanotechnologies, Sandia National Laboratories, Albuquerque, New
Mexico 87185, USA

⁴ School of Electrical and Computer Engineering, Purdue University, West Lafayette, Indiana
47907, USA

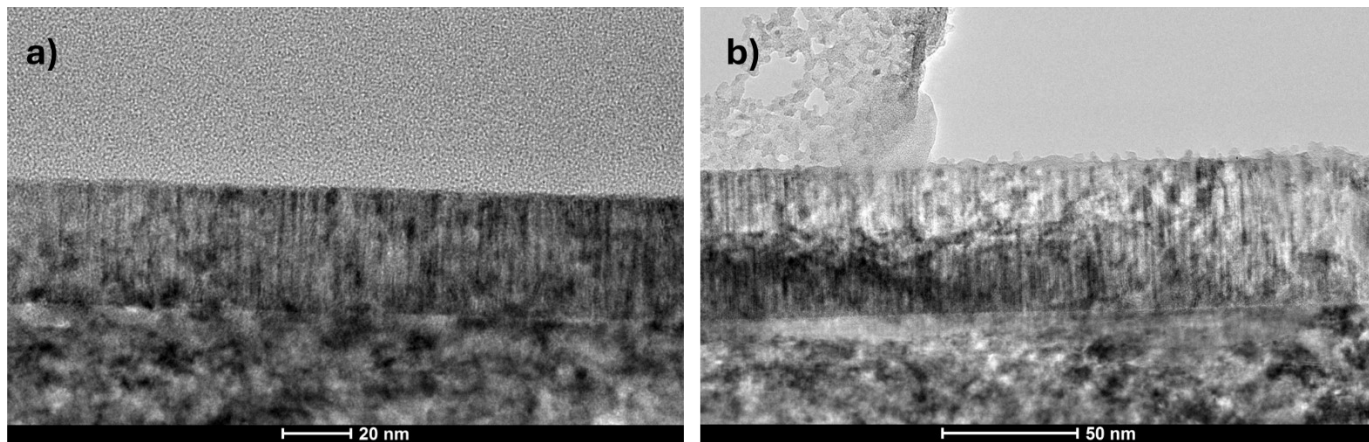
*Corresponding author: hwang00@purdue.edu



Supplementary Figure 1 X-ray diffraction (XRD) peak positions TiN-NiO thin films deposited at laser frequency of a) 2 Hz, b) 5 Hz, and c) 10 Hz on single-crystal MgO substrate.



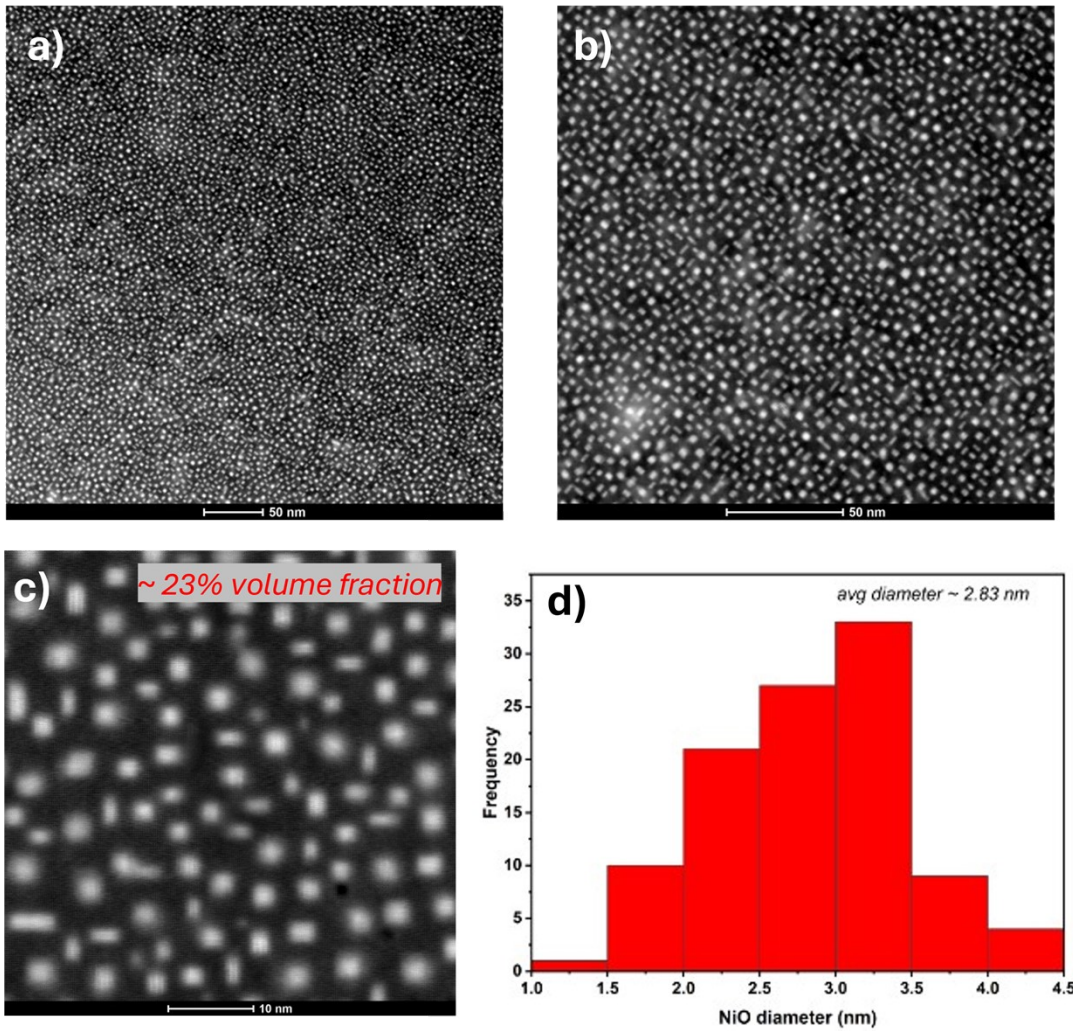
Supplementary Figure 2 Selected area electron diffraction (SAED) pattern of the TiN-NiO thin film deposited at a laser frequency of 5 Hz on an MgO substrate, showing the diffraction spots from the TiN matrix, NiO phase, and single-crystal MgO substrate, indicative of epitaxial or highly textured growth.



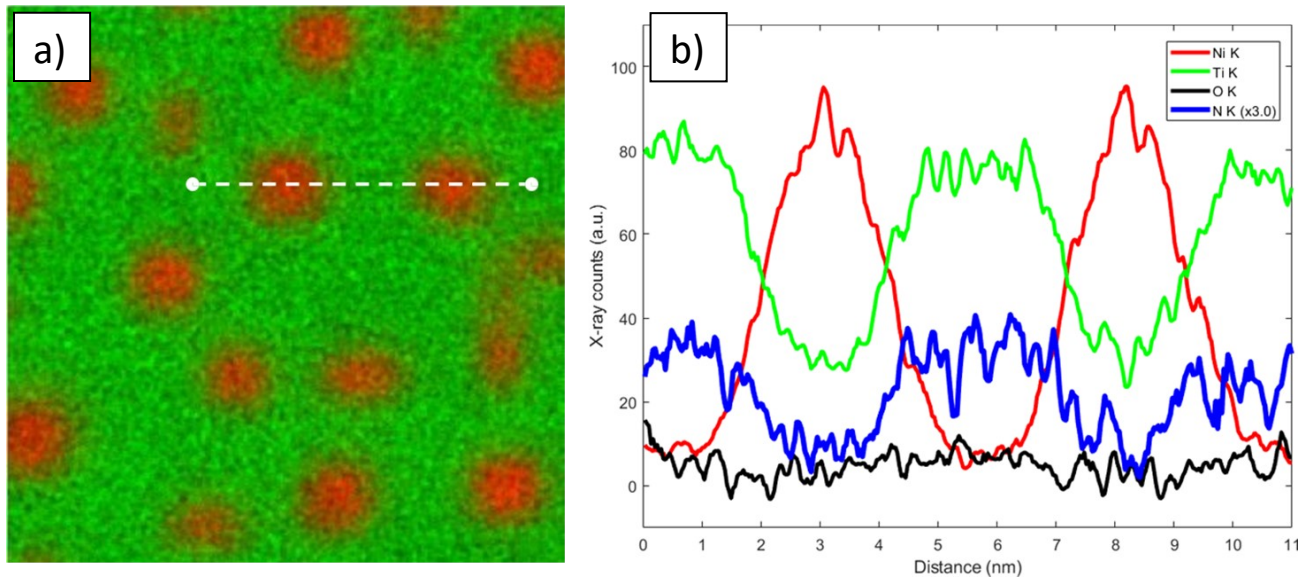
Supplementary Figure 3 Cross-section TEM images of TiN-NiO deposited at a) 5 Hz, and c) 2 Hz.

Table S1 Film thickness and estimated pillar areal density as a function of pulsed laser repetition rate.

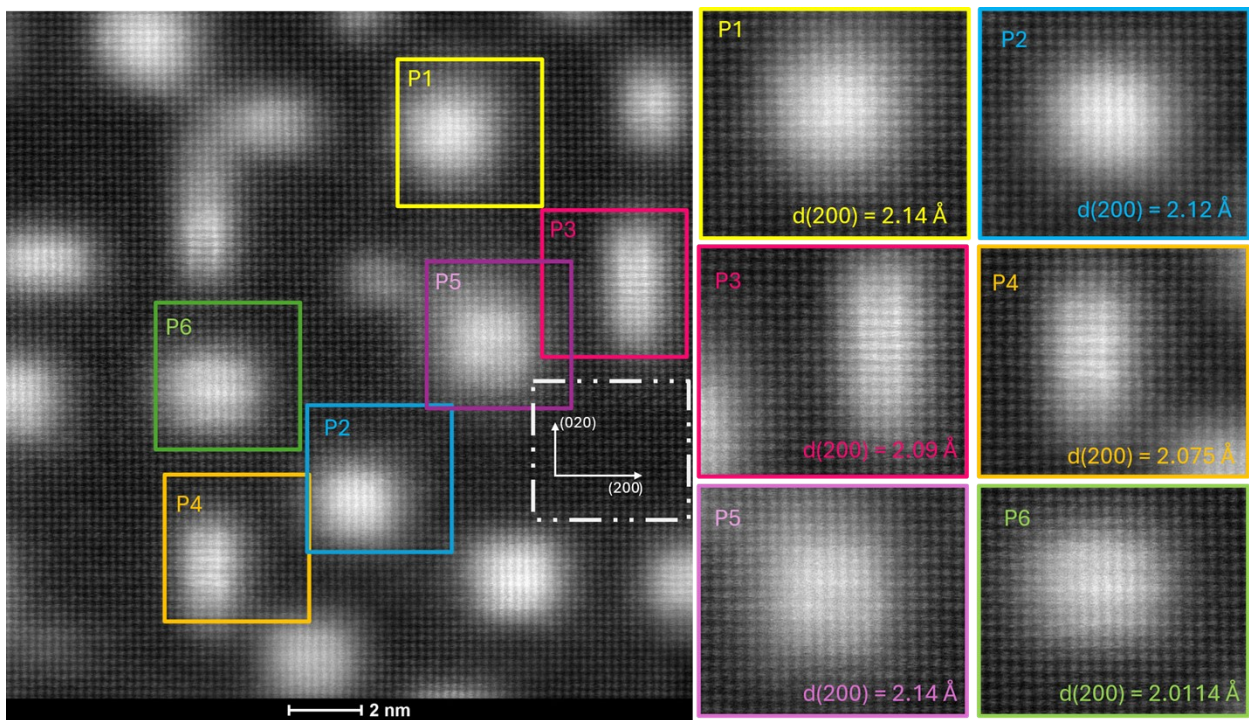
Laser frequency (Hz)	Thickness (nm)	Estimated pillar areal density
2	37	3.3×10^{12} pillars·cm ⁻²
5	56	4.8×10^{12} pillars·cm ⁻²
10	38	5.9×10^{12} pillars·cm ⁻²



Supplementary Figure 4 Plan-view TEM image of TiN-NiO thin film deposited at 5 Hz shown at a) low magnification, b) medium magnification, and c) high magnification, including a d) histogram of pillar diameter.



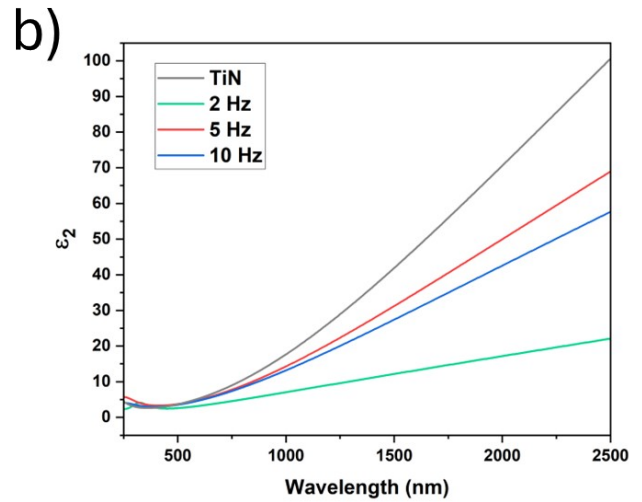
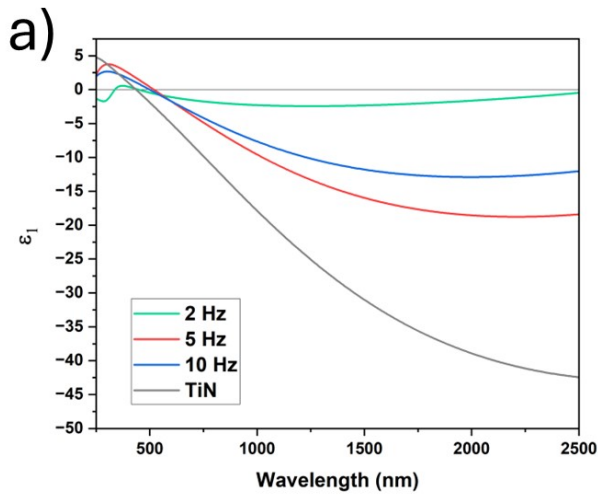
Supplementary Figure 5 a) EDS mapping of TiN matrix (green) and NiO (red) b) EDS line profiles of Ni, Ti, O, and N.



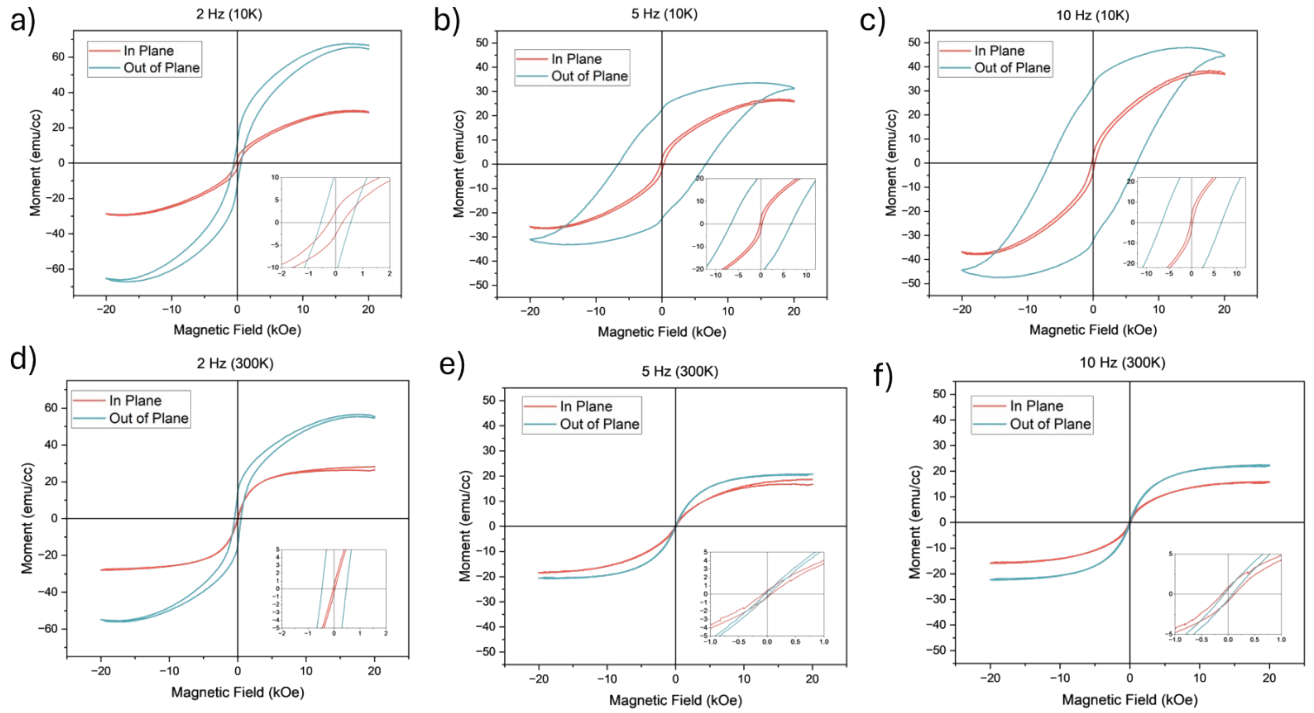
Supplementary Figure 6 Plan-view HRTEM lattice-fringe analysis of multiple NiO pillar regions in TiN matrix deposited at a laser frequency of 5 Hz (P1-6). Measurements were averaged over 7-15 consecutive lattice fringes per region of interest. The white border ROI represents the TiN matrix.

Table S2. In-plane lattice spacings measured from plan-view HRTEM.

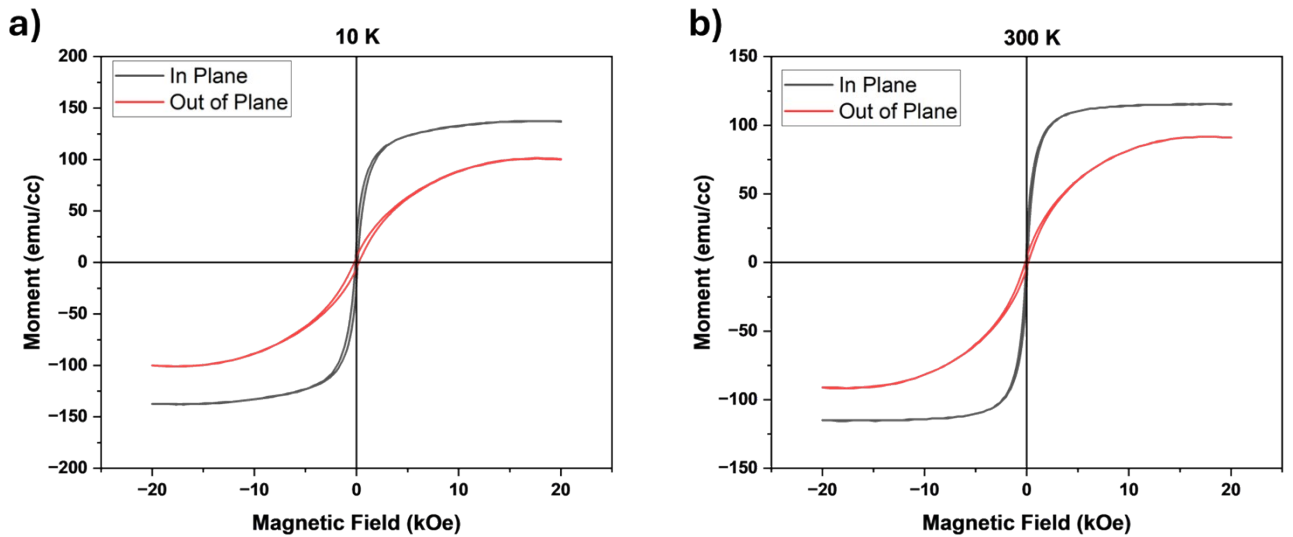
Pillar (#)	$d_{(200)}$ (Å)	$d_{(020)}$ (Å)	$a_{(200)}$ (Å)	$a_{(020)}$ (Å)
P1	2.148	2.059	4.297	4.11
P2	2.125	2.006	4.250	4.013
P3	2.096	2.042	4.193	4.084
P4	2.075	2.073	4.150	4.146
P5	2.140	2.064	4.285	4.129
P6	2.114	2.0125	4.229	4.025



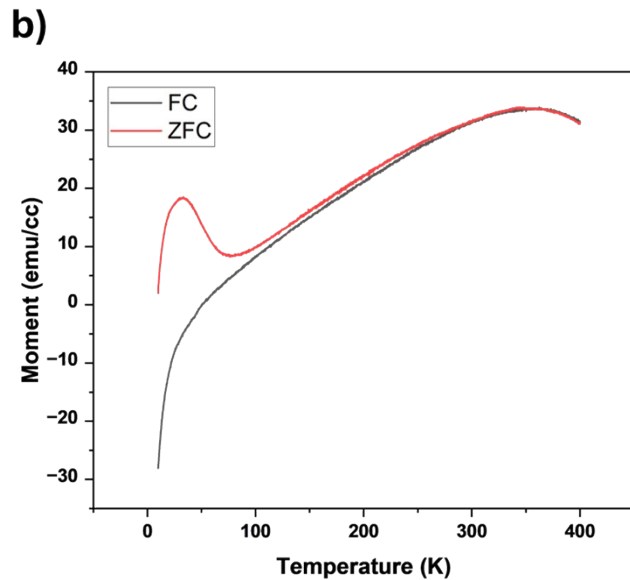
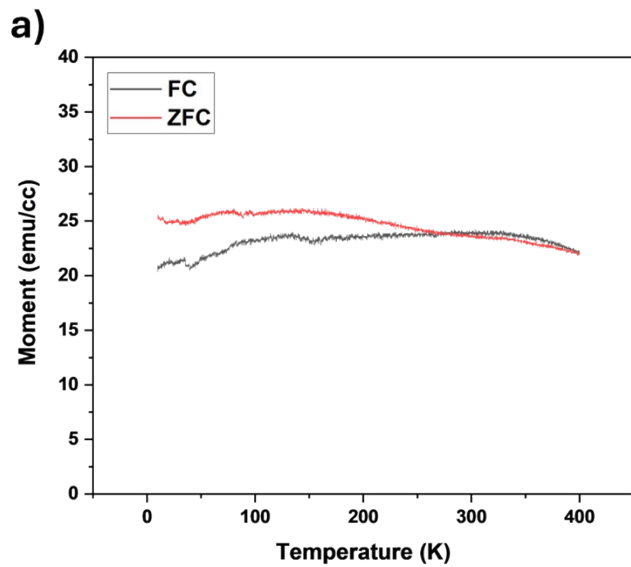
Supplementary Figure 7 In plane a) real and (b) imaginary part of the permittivity as a function of wavelength for TiN-NiO films deposited at laser frequency of 2, 5, and 10 Hz compared against a pure TiN thin film used as reference.



Supplementary Figure 8 Magnetic hysteresis loops of the TiN-NiO thin film deposited at laser frequencies of a) 2 Hz, b) 5 Hz, and 10 Hz measured at 10K and d) 2 Hz, e) 5 Hz, and f) 10 Hz measured at 300K.



Supplementary Figure 9 Magnetic hysteresis loops of TiN on MgO as a baseline measurement measured at a) 10 K, and b) 300 K



Supplementary Figure 10 Field-cooled (FC) and zero-field-cooled (ZFC) magnetization as a function of temperature for TiN-NiO thin film deposited at a) 5 Hz and b) 10 Hz, measured under a constant applied magnetic field.